algorithms

MDPI

Article

An Innovative Mathematical Model of the Spine: Predicting Cobb and Intervertebral Angles Using the 3D Position of the Spinous Processes Measured by Vertebral Metrics

Ana Teresa Gabriel [1,2,*], Cláudia Quaresma [3] and Pedro Vieira [4]

[1] UNIDEMI, Department of Mechanical and Industrial Engineering (DEMI), Faculty of Sciences and Technology, NOVA University Lisbon, 2829-516 Caparica, Portugal
[2] LASI, Intelligent Systems Associate Laboratory, 4800-058 Guimarães, Portugal
[3] LIBPhys—UNL, Laboratory for Instrumentation, Biomechanical Engineering and Radiation Physics, Faculty of Sciences and Technology, NOVA University Lisbon, 2829-516 Caparica, Portugal; q.claudia@fct.unl.pt
[4] Faculty of Sciences and Technology, NOVA University Lisbon, 2829-516 Caparica, Portugal; pmv@fct.unl.pt
* Correspondence: a.gabriel@fct.unl.pt

Abstract: Back pain is regularly associated with biomechanical changes in the spine. The traditional methods to assess spine biomechanics use ionising radiation. Vertebral Metrics (VM) is a non-invasive instrument developed by the authors in previous research that assesses the spinous processes' position. However, the spine model used by VM is not accurate. To overcome it, the present paper proposes a pioneering and simple articulated model of the spine built through the data collected by VM. The model is based on the spring–mass system and uses the Levenberg–Marquardt algorithm to find the arrangement of vertebral bodies. It represents the spine as rigid geometric transformations from one vertebra to the other when the extremity vertebrae are stationary. The validation process used the Bland–Altman method to compare the Cobb and the intervertebral angles computed by the model with the radiographic exams of eight patients diagnosed with Ankylosing Spondylitis. The results suggest that the model is valid; however, previous clinical information would improve outcomes by customising the lower and upper vertebrae positions, since the study revealed that the C6 rotation slightly influences the computed angles. Applying VM with the new model could make a difference in preventing, monitoring, and early diagnosing spinal disorders.

Keywords: spine biomechanics; mathematical model; Cobb angles; intervertebral angles; Vertebral Metrics

Citation: Gabriel, A.T.; Quaresma, C.; Vieira, P. An Innovative Mathematical Model of the Spine: Predicting Cobb and Intervertebral Angles Using the 3D Position of the Spinous Processes Measured by Vertebral Metrics. *Algorithms* **2024**, *17*, 134. https://doi.org/10.3390/a17040134

Academic Editors: Alicia Cordero and Juan Ramón Torregrosa Sánchez

Received: 5 February 2024
Revised: 18 March 2024
Accepted: 20 March 2024
Published: 25 March 2024

1. Introduction

Poor posture is often associated with a lack of postural control. It provides an unstable connection between the body's segments and unexpected strains on the supporting structures [1–3]. As such, it may represent a risk of back pain and disorders [4].

The World Health Organization outlines back pain as one of the most common health problems worldwide [5]. It is a leading cause of absenteeism at work [6] and significantly impacts personal, social, and government levels [7–9].

The spine is mobile in all three axes of the cartesian coordinate system as a translation or a rotation [10–12]. However, there is variability in mobility between spinal regions since movement between adjacent vertebrae is limited. Nevertheless, even small movements in one direction can provide an extensive range of motion to the global spine [11].

The cervical, thoracic and lumbar vertebrae are interconnected by fibrocartilaginous intervertebral discs [13]. Except for the atlas and axes, vertebrae share a typical structure, which includes the vertebral body and the arch. The vertebral body is the cylindrical part of the vertebra. The latter is the lateral and posterior aspects of the vertebra, consisting of paired pedicles and laminae, which join posteriorly, forming the spinous process [11,12]. The apex of each vertebra is a cutaneous prominence visible along the back midline [14].

Pathological conditions or disorders may change the spine's biomechanics [12,15], compromising the spinal alignment [16].

The quantitative evaluation of spine biomechanics is crucial to managing medical procedures. Radiological techniques are the most widely used for these purposes despite their association with ionising radiation [17–19]. Other conventional 3D imaging techniques, such as magnetic resonance imaging (MRI), require the patient to lie down, and many spinal deformations are lost [20]. On the other hand, non-invasive tools are not standard in clinics [21]. Some do not allow 3D analysis [22,23], while others only assess partial segments [24,25] or require contact points during evaluation [26]. Despite its ability to perform a biomechanical assessment of the spine, technologically advanced instruments, such as optical systems, have limitations, such as the background or lighting conditions [3,27].

Our research team developed the Vertebral Metrics (VM) tool in previous research. It is a patented device (patents PT/103990, PCT/IB2009/005018, and US20110004125) that was designed to identify the spinous processes' apex position without ionising radiation [28]. As such, it combines a stereo vision system with software that recognises fluorescent marks in the skin [29,30]. The device was developed, and the measurement resolution was determined [30]. Nevertheless, to assess the spine biomechanics, a model of the spine based on the apex position must be used. The previous model only provided the spine overview in the sagittal plane, so the information was insufficient and needed to be more comprehensive. Moreover, it only used one spring to simulate each intervertebral disk, which allows more degrees of freedom than the anatomical possibilities [29]. Therefore, the authors improved the concept and proposed a new mathematical model in the present paper.

Modelling the spine is complex [31]. It may explain why the literature only describes a few studies, with most focusing only on the lumbar spine [32,33].

The mathematical models can be continuous or discrete parameters. The first type is recommended as a first approximation because it does not consider mobility constraints [10,32,34]. The discrete type considers every single element. Generally, they represent the vertebrae by rigid bodies, whereas the ligamentous structures, muscles, or articulating facets are massless springs [34]. However, most discrete models use approximations of image techniques such as X-ray, magnetic resonance, or computer tomography [33,35,36].

This paper describes the new and innovative discrete model that uses the apex of the spinous processes measured by VM to estimate the vertebrae's position between S1 and C6 and assess the spine biomechanics in the three planes.

2. Methods

This study uses the data collected by the VM as a reference to find the arrangement of the vertebral bodies, the Cobb angles, and the intervertebral angles between S1 and C6.

The model was developed in MATLAB® (R2016b version). As in discrete model types, the spine is compared to a system of interconnected masses and springs. Each mass is a vertebral body, while each intervertebral disc is represented by three springs (A, B, and C, as shown in Figure 1). Their connection points differ 120 degrees from the geometric centre of the masses' surface.

By modelling each intervertebral disk using three springs, the degrees of freedom are reduced compared with the previous model used by VM. Also, any torsional or shift movement of 2 consecutive vertebrae will change the springs' length and, consequently, their energy.

Between S1 and C6, the spine presents 20 vertebrae and 19 intervertebral discs. According to the authors' convention, the first mass is S1, while the last is C6. Similarly, the first group of three springs is the intervertebral disc between L5 and S1.

The following subsections provide a detailed description of each step underlying the developed model.

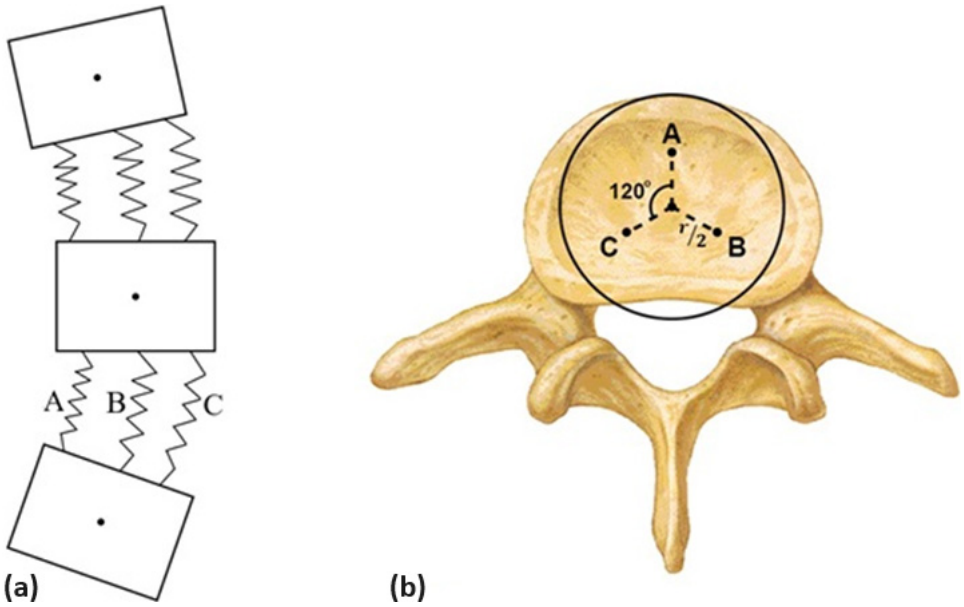

Figure 1. (**a**) Sketch of the system of masses and springs; (**b**) the springs' position in the end plate. A, B and C are the connection points of the three springs.

2.1. Establishing Input Conditions

In the first step, input conditions were established. These included pre-defined anatomical and physical characteristics. Respect for the anatomical differences between vertebrae and intervertebral discs is relevant to the relationship between rigid and elastic elements.

Regarding the anatomical properties, the statistical dimensions and orientation of the vertebrae were obtained from the literature and are presented in Table 1 [37–39]. For a better understanding, Figure 2 provides the vertebrae components and measures considered in different perspectives.

Table 1. Vertebrae's characteristics [37–39].

	S1	**L5**	**L4**	**L3**	**L2**	**L1**	**T12**	**T11**	**T10**	**T9**	**T8**	**T7**	**T6**	**T5**	**T4**	**T3**	**T2**	**T1**	**C7**	**C6**
EPW (mm)	48	48	48	46	44	42	42	39	35	33	30	29	28	27	26	26	27	28	23	20
EPD (mm)	34	34	35	35	35	35	33	32	32	31	29	28	27	26	24	23	22	20	18	17
EPA (mm^2)	-	1218	1273	1290	1197	1117	1024	945	834	754	664	603	552	495	444	412	400	376	280	290
VBH (mm)	23	23	24	24	24	24	23	21	20	19	19	18	17	16	16	16	16	14	13	11
SCW (mm)	-	27	25	24	24	24	22	19	18	18	18	17	17	17	17	18	19	22	25	26
SCD (mm)	-	20	19	17	18	19	18	16	15	16	16	16	16	16	16	16	15	16	15	15
PDW (mm)	-	16	14	10	8	9	9	10	9	8	7	6	6	6	6	7	8	8	7	6
PDH (mm)	-	16	15	14	15	16	17	16	15	14	12	12	12	11	12	12	11	10	7	7
PDIt (°)	-	5	4	3	3	3	5	9	7	8	12	11	8	8	8	9	8	8	11	6
SPW (mm)	5	5	6	7	6	7	5	5	5	5	5	4	4	5	4	5	5	7	6	7
SPD (mm)	27	31	32	33	30	27	27	25	27	30	34	35	35	35	33	32	30	30	30	25
SPH (mm)	10	14	15	14	14	15	15	10	11	9	9	9	8	8	9	9	8	10	8	7
SPIt (°)	10	19	11	13	11	10	2	10	25	29	45	54	57	61	53	38	30	20	20	20

EPW—end-plate width; EPD—end-plate depth; EPA—end-plate area (inferior); VBH—vertebral body height; SCW—spinal canal width; SCD—spinal canal depth; PDW—pedicle width; PDH—pedicle height; PDIt—pedicle inclination (transverse plane); SPW—spinous process width; SPD—spinous process depth; SPH—spinous process height; SPIt—spinous process inclination (transverse plane).

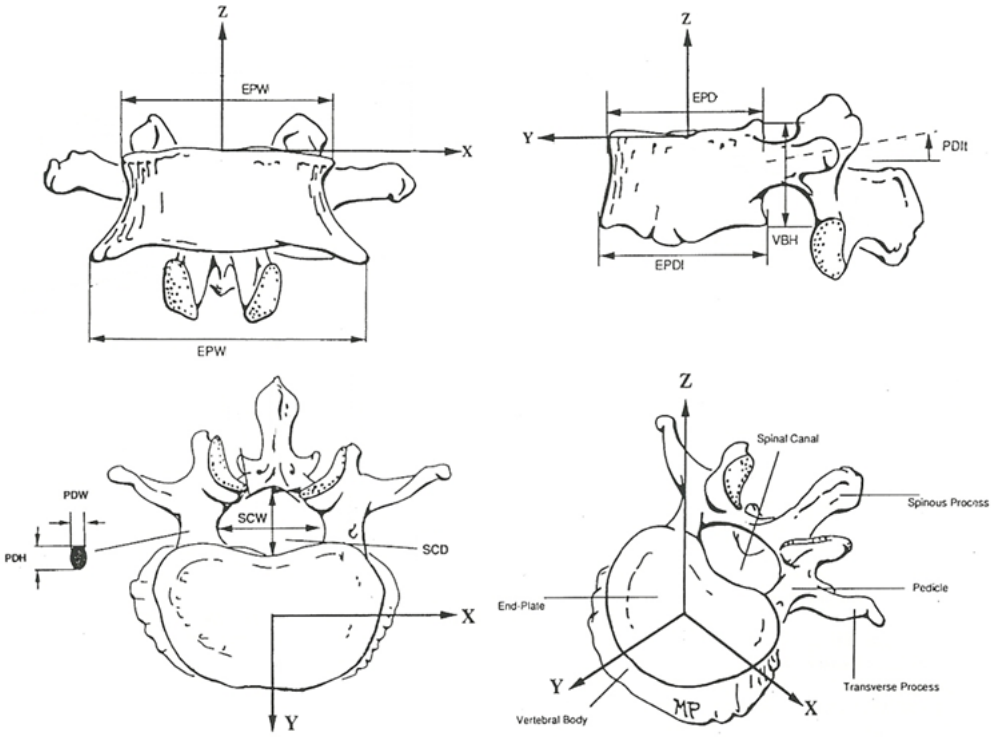

Figure 2. Anatomy of a lumbar vertebra [39].

The characteristics considered for the intervertebral disks are presented in Table 2.

Table 2. Intervertebral disks' characteristics [37–39].

	S1–L5	L5–L4	L4–L3	L3–L2	L2–L1	L1–T12	T12–T11	T11–T10	T10–T9	T9–T8	T8–T7	T7–T6	T6–T5	T5–T4	T4–T3	T3–T2	T2–T1	T1–C7	C7–C6
IDH	9	9	9	9	9	5	5	5	5	5	5	5	5	5	5	5	5	3	3
k (N/mm)	683	714	724	672	627	1034	954	842	762	671	609	558	500	448	416	404	380	471	488

IDH—intervertebral disk height; k—constant factor (stiffness) estimated for the intervertebral disk.

The previous information is for an average height of 167.8 cm [37].

Another consideration taken in the present model is that the alignment of the vertebrae along the spine would provide the minimum potential energy to the whole system. The Levenberg–Marquardt (LM) algorithm solves this optimisation problem [40].

The energy of each intervertebral disc is the sum of the potential elastic energy of the three springs. To find the total potential energy (*TPE*) of the system, the potential elastic energy of all intervertebral discs is added, as shown below.

$$TPE = \sum_{i=1}^{23} 1/2k_i \left[(\Delta l_A)_i^2 + (\Delta l_B)_i^2 + (\Delta l_C)_i^2 \right]$$

As mentioned in Table 2, k_i is the stiffness of the intervertebral disc, which is the same for springs *Ai*, *Bi*, and *Ci*. Δl is the change in the spring size. The height of the correspondent disc gives the initial size and is equal to springs *Ai*, *Bi*, and *Ci*.

In the coordinated system adopted, X is the transversal axis, Y represents the antero-posterior axis, and Z is the vertical axis [30].

Constraints were also included regarding the maximum rotation of the vertebrae in the sagittal plane (±75°) and in the transversal plane (±45°). Those values are extreme enough; however, they include all the rotation possibilities.

2.2. Estimating the Spine Biomechanics

The main steps to build the model were as follows:

1. Definition of an initial spring–mass system;
2. Match the initial system and the VM data;
3. Modulation in the sagittal plane;
4. Modulation in the coronal plane;
5. Find the Cobb and the intervertebral angles;
6. Three-dimensional representation.

The following subsections describe these steps.

2.2.1. Defining an Initial Spring–Mass System

Despite its unreal anatomical characteristics, the initial system represents the arrangement of the masses when the springs are at their initial size and the upper and lower surfaces of all masses are parallel. As such, springs A, B, and C have the same size. Figure 3a shows the initial system. The cobblestones represent the masses, while the + marks its apex.

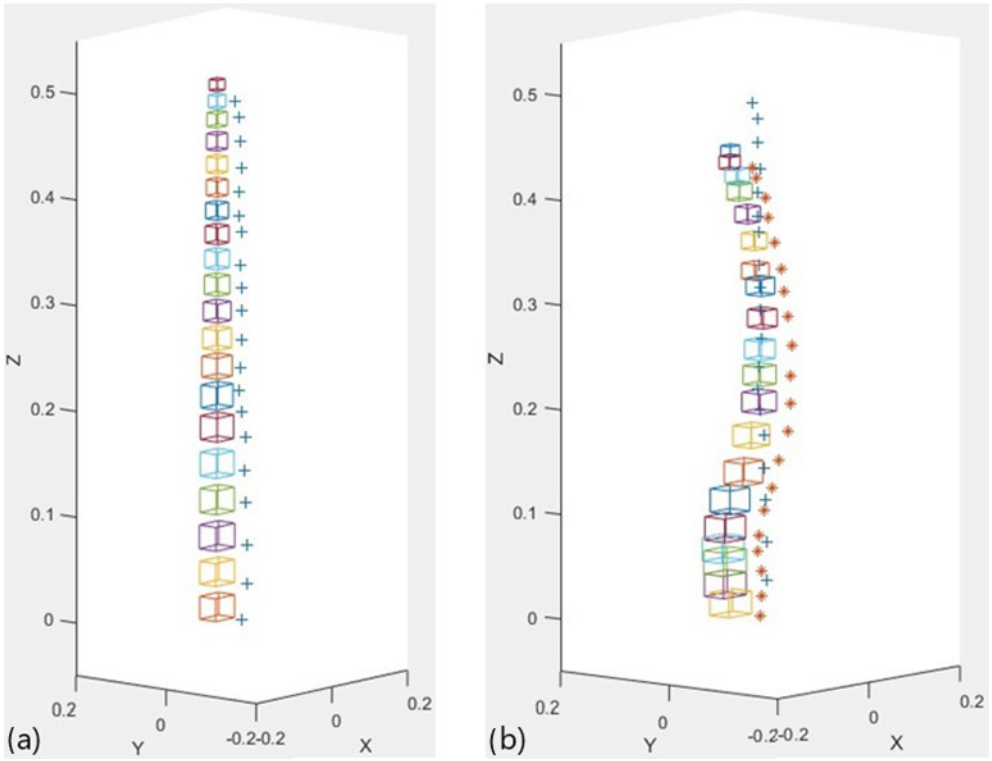

Figure 3. (**a**) Alignment of the initial system; (**b**) matching the data acquired by VM.

2.2.2. Matching the Initial System and VM Data

In this stage, the algorithm adjusts the initial system to the VM data. It performs translations of the rigid elements so that each apex matches the positions provided by the VM. Figure 3b presents an example. The + symbol is the apex of the spinous processes of the initial system, while * is the apex identified by the VM.

The previous movement unbalances the system since the springs are compressed or stretched compared to their initial position. The masses may even overlap, which is anatomically impossible. This problem is solved in the next phase by modelling in the sagittal and transversal planes.

2.2.3. Modelling in the Sagittal Plane

The differences regarding the initial position are the most evident in the sagittal plane. As a result, the modelling process starts in this plane.

First, S1 and C6 assume the rotation provided by the literature: −42.46° and −16.20°, respectively [37,39]. It cannot change in future steps to guarantee the spine pattern. Then, the model uses the LM algorithm to adjust the other masses simultaneously, but it limits the rotation angles according to the constraints previously described. Once the best adjustment is found, the rotation matrix calculates the 3D position of each mass.

As a result of the modelling, the masses align. Notably, they do not overlap in the sagittal plane. Figure 4a presents an example of the alignment after modelling in the sagittal plane.

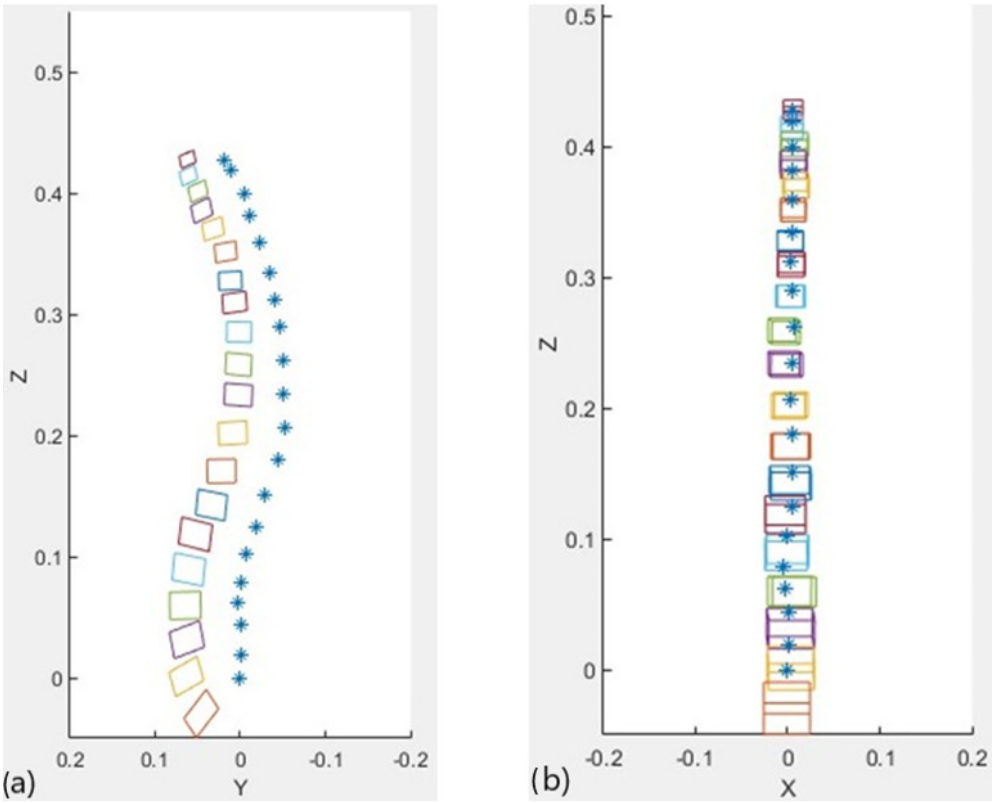

Figure 4. Vertebrae alignment in the (**a**) sagittal plane; (**b**) transversal plane.

2.2.4. Modeling in the Transversal Plane

This step aims to find the rotation angle of each mass in the transversal plane that minimises the total potential elastic energy.

The same approach described in the previous step was adopted here, except that the model does not force S1 and C6 to a fixed rotation (their initial rotation is 0°). It happens because rotations in the transversal plane are not so evident as in the sagittal plane. The variables optimised by the LM algorithm represent the axial rotation angles of each mass.

Figure 4b shows the system after this step. Although the vertebrae seem to overlap, it is an illusion caused by the sagittal rotation angle.

2.2.5. Cobb Angles and Intervertebral Angles

The following vertebrae contribute to finding the Cobb angles:

- L1 and S1 to the lumbar lordosis;
- D1 and D12 to the dorsal kyphosis;
- C2 and C7 to the cervical lordosis.

For the lumbar lordosis, for example, the lower limit vertebra (LLV) is S1, while the upper limit vertebra (ULV) is L1.

The process finds a vector parallel to the bottom surface of the LLV and another vector parallel to the upper surface of the ULV. The angle between the two vectors is the Cobb angle (grey colour in Figure 5a).

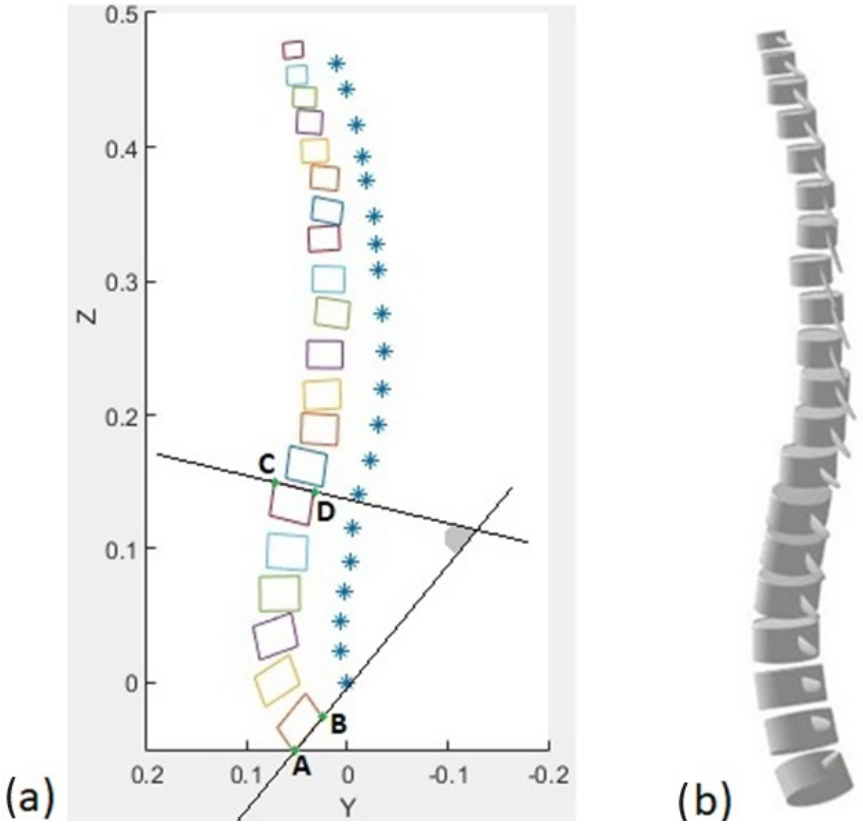

Figure 5. (**a**) Angle of lumbar lordosis (Cobb angle); (**b**) 3D representation of the spine.

The process to calculate the intervertebral angles is the same but uses consecutive vertebrae.

2.2.6. 3D Representation

The 3D representation of the spine is shown in the user interface of the VM system. Solid Constructive Geometry and Description of Surfaces were the combined MATLAB® methods used to implement this tool.

A cylinder represents the vertebral body, while each spinous process is a cylinder with a spherical tip. All vertebrae are positioned so that the relative position between their apex matches the data acquired by the VM, and their vertebral bodies have the alignment found by the mathematical model.

Figure 5b shows a graphical example. The user can rotate, zoom, or drag the image in the user interface.

2.3. Testing and Validation

Testing the integrated system's performance was a preliminary task of an extensive research project developed in a partnership between this research team, the NOVA Medical School research center, and the Rheumatology Service of a referral hospital in Lisbon, Portugal.

This preliminary study included eight patients diagnosed with AS. The inclusion criteria were precise, which limited the sample size, and included the following requirements:

- Age over 18 years old;
- Diagnosis of Ankylosing Spondylitis according to the Modified New York criteria [41–43];
- Body mass index below 35 kg/m^2;
- No pregnancy or breastfeeding;

- No infections requiring hospitalisation or antibiotics;
- No uncontrolled medical illness;
- No total ankylosis of the spine;
- X-rays of the spine in the sagittal and coronal planes;
- Radiographs taken within less than two years since the biomechanical changes in the spine are insignificant during a shorter period [44,45].

The institutional Medical Ethics Review Board granted ethical approval. All subjects read written information about the aims and plans of the study. A brief questionnaire, including biographic and biometric details, was completed, and all patients signed a consent form before data collection.

Some requirements were established to reduce the effect of external variables and guarantee the comparability of the measures:

- The same physician identified the cutaneous projection of the apex through palpatory anatomy;
- The same researcher carried out data collection;
- The sampling method was random.

Nine consecutive measurements with VM were carried for each patient. As the inclusion criteria, the number of measures respected the requirements of the global study, which included the analysis of postural adjustments using the VM as the assessment tool. The nine measurements were performed with a single fluorescent marking procedure.

The model fixed the rotation angles of C6 and S1 according to the values found in the literature.

New devices for application in clinics must be validated through comparison with the gold standard techniques. For this reason, after data collection, the results were carefully compared with the patient's radiographs.

Regarding the analysis of the radiographs, Adobe Photoshop CC 2015® was used to measure the proper angles. The same evaluator performed the multiple steps involved. In each radiograph and for each vertebra, the following parameters were identified:

- The upper limits of the surfaces of the vertebral body;
- The lower limits of the surfaces of the vertebral body;
- The upper and lower limits of the apex.

The previous parameters were used in the Cobb method [46] to find the amplitude of the dorsal kyphosis, the lumbar lordosis, and the intervertebral angles.

Together with the data provided by the mathematical model, this information was processed using SPSS® (version 20.0).

The Bland–Altman method was applied to compare the data [47,48]. It is based on a plot analysis and it is adequate "to evaluate a bias between the mean differences, and to estimate an agreement interval, within which 95% of the differences of the second method, compared to the first one, fall" [49]. The choice for the validation method is also supported by the following facts: (i) it is one of the most used methods to investigate the agreement between different approaches that provide the same measure and it is especially common for studies within the clinical context [50–55]; (ii) the measuring principles underlying the VM device were validated using the same method [46].

3. Results

The age of the eight patients included in the study ranged from 22 to 55 years old.

Figures 6a and 7a show the results of the Bland–Altman analysis for the dorsal kyphosis and lumbar lordosis, respectively. Very few observations are outside the 95% confidence interval (three in kyphosis and two in lordosis).

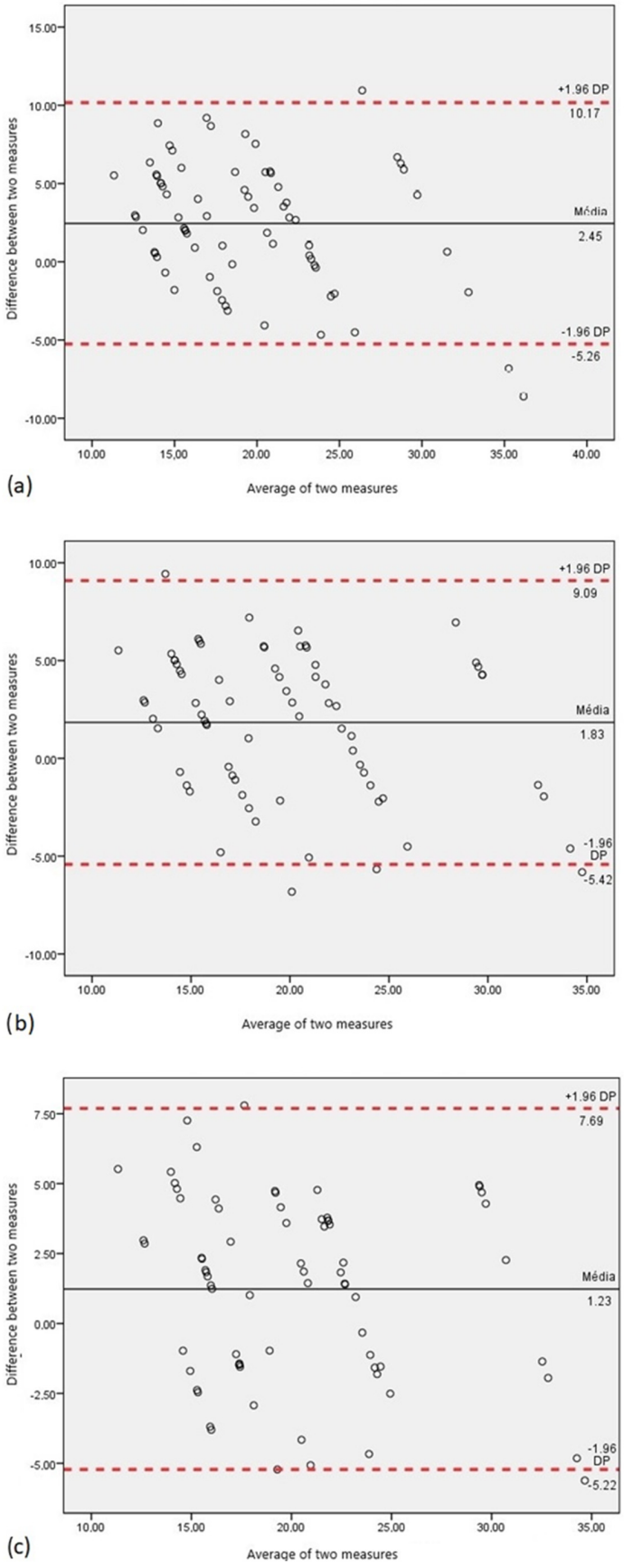

Figure 6. Bland–Altman analysis for the dorsal kyphosis using the rotation angle of C6 given by (**a**) the literature, (**b**) the average value; (**c**) the value measured in each radiograph.

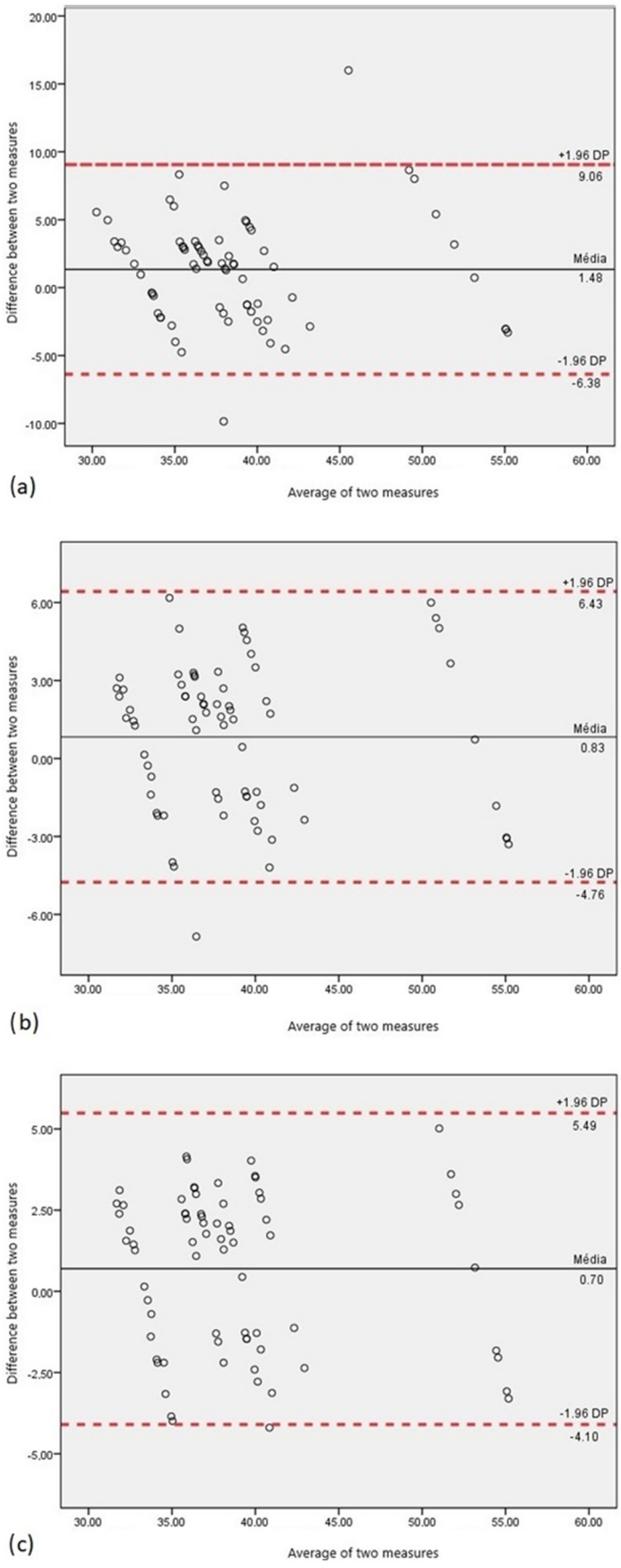

Figure 7. Bland–Altman analysis for the lumbar lordosis using the rotation angle of C6 given by (**a**) the literature, (**b**) the average value; (**c**) the value measured in each radiograph.

Although the values outside the confidence interval are possible outliers, they can also be related to the rotation angle of C6. In addition to C6 in a high mobility region, the literature value is used regarding a population without spinal pathologies.

Thus, the model was applied, considering that the C6 rotation angle is given by the following information:

1. The average of the rotation angles measured on the eight radiographs;
2. The angle measured on the radiograph of each patient.

Figures 6b and 7b show the Bland–Altman analysis for case 1. Some observations are still outside the 95% confidence interval; however, they are closer to it.

Figures 6c and 7c show the Bland–Altman analysis for case 2. For both dorsal kyphosis and lumbar lordosis, the results improved significantly. In the first curvature, the outside observations are closer to the 95% confidence interval, whereas only one value is at the limit of the 95% confidence interval for the second curvature.

The three approaches to the C6 rotation regarding the intervertebral angles were also analysed.

Most of the observations are within the 95% confidence interval. In addition, a pattern that points to the spine regions with more (or less) relevant differences was not found.

4. Discussion

The following characteristics must be considered to model the biomechanics of the spine: its linear geometry, the joints at each intervertebral level, and its multiaxial movements [32]. Therefore, the mathematical model developed within this study uses an articulated model.

As previously mentioned, articulated models represent the spine as rigid geometric transformations from one vertebra to the other. Typically, in these types of models, the first vertebra is stationary, while the previous ones guide each successive vertebra [20].

However, the methodology to find the minimum energy for the spring–mass system required that the position of the two extremity vertebrae was pre-determined and fixed.

As a result, the mathematical model uses an articulated spine model that can include 20 masses (from S1 to C6) and requires a reference point by each vertebra: the apex of its spinous process previously identified by the VM.

A preliminary study evaluated the capability to quantify the Cobb and intervertebral angles. The Cobb angles are the gold standard parameter to evaluate spinal biomechanics. On the other hand, the intervertebral angles are not a standard, but they can be used to evaluate the model's performance compared to the radiographs.

Height patients of a Portuguese hospital with ages ranging from 22 to 55 years old participated in the study. Although the biomechanical changes in the spine are more prone to happen with age, they are a consequence of modifications in the vertebrae alignment. The biomechanical spinal changes affect the vertebrae positioning and, consequently, the spinous processes' positioning. By identifying the 3D position of their apex, we were able to model the vertebrae configuration independently of their age.

The integrated system (VM and the new mathematical model) identified and modelled the 20 vertebrae.

The results suggest that the position of C6 in the sagittal plane slightly influences the model performance. The 95% confidence interval limits decreased by customising the C6 rotation angle for each patient according to the radiographic data. This is because the literature did not include the effects of Ankylosing Spondylitis or the inter-individual variability.

Note that the errors associated with the measuring of the 3D position of the fluorescent marks were already quantified in previous studies performed by the authors Gabriel et al. in 2015; Gabriel et al. in 2018. The mentioned studies focused on the development and validation of the measuring performance of the VM device. It was statistically proven to provide accurate results (errors in the order of 1 mm). The resolution in the order of 1 mm is satisfactory since this value is much smaller than the diameter of the fluorescent marks (around 3 mm), as well as smaller than the anatomical dimension of the spinous processes.

A previous study measured the height of the spinous processes (vertical distance between their upper and lower edges) of L1, third lumbar vertebra (L3) and L5 in 15 patients. The average height found for each of the spinous processes was 20.5 mm, 20.2 mm and 14.1 mm, respectively [19]. Although this parameter is conditioned by several factors (such as the type of vertebra, genetics and associated pathologies), it always exceeds 1 mm, meaning that the VM measurement error does not compromise the measure of the 3D position of the spinous processes.

Regarding the mathematical model presented in the current paper, we focused on the analysis of the differences between the angles provided by the model and the angles measured in the radiographs. The Bland–Altman plot analysis "only defines the intervals of agreements, it does not say whether those limits are acceptable or not. Acceptable limits must be defined a priori, based on clinical necessity, biological considerations or other goals" [49]. This project was carried out in collaboration with the rheumatologic department of a Portuguese hospital, which provided insightful feedback of the results. From a clinical point of view, the number of points outside the 95% confidence interval are not meaningful especially because they can be influenced by the error introduced by the fluorescent marking process. It is noteworthy that the person that performs the fluorescent marking process must be an expert to reduce the possibility of error.

Overall, the results of the Bland–Altman methodology show that the model can be a reliable and valid method compared to radiography. It encourages future steps, including adjusting the coronal plane and validating the integrated system.

Compared to the previous mathematical model developed for VM, the new model seems to be closer to reality, being the only model that actually presents results in more than one plane [29]. In addition, it is the first model that provides information about the amplitude of intervertebral angles.

Nevertheless, some limitations exist. Finding a large sample without pathology is a substantial concern since radiographs must have a clinical reason in Portugal. Another problem is the lack of distinct patterns of spine biomechanics both for healthy populations and those with disorders/pathologies. In addition, it is important to note that the main objective of our study was to analyse certain aspects of the dynamic behavior of the spine, rather than replicate all the biomechanical complexities found in the human body.

To summarise, the first evaluation of the spinal model developed in this work was a success and demonstrated its potential to study populations with and without pathology. We genuinely believe that it is an asset to VM.

5. Conclusions

Biomechanical changes in the spine are a common symptom in today's society and a leading cause of back pain. Although any individual may experience back pain, age, posture, and lifestyle have been identified as risk factors.

The literature reflects the lack of studies about the biomechanical changes in the spine. The difficulty of carrying out quantitative measures may justify this lack of studies since most techniques, including radiography (gold standard), are invasive.

The lack of non-invasive techniques to quantify the biomechanical changes in the spine led to this research team's development of the VM. The device was designed to evaluate the spine based on the spinous processes' 3D apex position.

The spinal model developed within the scope of this project revealed encouraging results. Furthermore, these results can be improved when anatomical patterns of the spine become available because the anatomical characteristics used here reflect the population 30 decades ago. Understanding anatomical variability and its relationship with individual factors such as sex, height, ethnicity, and even pathologies would be remarkable for this area. A faster solution may include applying a complementary technique, such as ultrasound, to estimate the angle of rotation of the extremity vertebrae in the sagittal plane. Alternatively, it can be measured from previous radiographs.

As far as the literature is concerned, this is the first mathematical model that features the spine using the apex as the reference point. Also, it is the first model that has been directly implemented in the VM software, which significantly improves the device.

A promising perspective of this pioneering system is the longitudinal analysis of patients. Periodical evaluations could be helpful to prevent, monitor, or even understand the progression patterns instead of diagnosing already changed modes. It could be a significant breakthrough in the health area since patients with severe progression disorders could be followed more closely. Moreover, patients with lower progression risks could receive less aggressive treatments.

Author Contributions: Conceptualization, A.T.G., C.Q. and P.V.; methodology, A.T.G.; software, A.T.G.; validation, A.T.G., C.Q. and P.V.; formal analysis, A.T.G.; investigation, A.T.G.; resources, A.T.G., C.Q. and P.V.; writing—original draft preparation, A.T.G.; writing—review and editing, C.Q. and P.V.; supervision, C.Q. and P.V.; project administration, P.V. All authors have read and agreed to the published version of the manuscript.

Funding: This research received no external funding.

Data Availability Statement: Data are unavailable due to privacy and ethical restrictions. Nevertheless, the authors are available to respond to reasonable requests or questions regarding the algorithm (a.gabriel@fct.unl.pt).

Acknowledgments: The authors acknowledge Fundação para a Ciência e a Tecnologia (FCT-MCTES) for its financial support via the project UIDP/00667/2020 and UIDB/00667/2020 (UNIDEMI). Research was also supported by Fundação para a Ciência e a Tecnologia through research Grants UIDB/FIS/04559/2020 and UIDP/FIS/04559/2020 (LIBPhys) and LASI-LA/P/0104/2020 (LASI), from FCT/MCTES, Portugal.

Conflicts of Interest: The authors declare no conflicts of interest.

References

1. American Academy of Orthopaedic Surgeons. *Posture and Its Relationship to Orthopaedic Disabilities—A Report of the Posture Committee*; American Academy of Orthopaedic Surgeons: Evanston, IL, USA, 1947.
2. Magee, D.J. *Orthopedic Physical Assessment*, 4th ed.; Saunders Company: New York, NY, USA, 2002.
3. Aroeira, R.M.C.; de Las Casas, E.B.; Pertence, A.E.M.; Greco, M.; Tavares, J.M.R. Non-invasive methods of computer vision in the posture evaluation of adolescent idiopathic scoliosis. *J. Bodyw. Mov. Ther.* **2016**, *20*, 832–843. [CrossRef] [PubMed]
4. Singla, D.; Veqar, Z. Effect of playing basketball on the posture of cervical spine in healthy collegiate students. *Int. J. Biomed. Adv. Res.* **2015**, *6*, 133–136. [CrossRef]
5. Ehrlich, G.E. Low back pain. *Bull. World Health Organ.* **2003**, *81*, 671–676. [PubMed]
6. Dionne, C.E.; Dunn, K.M.; Croft, P.R. Does back pain prevalence really decrease with increasing age? A systematic review. *J. Am. Geriatr. Soc.* **2006**, *35*, 229–234. [CrossRef] [PubMed]
7. Hoy, D.; Brooks, P.; Blyth, F.; Buchbinder, R. The Epidemiology of low back pain. *Best Pract. Res. Clin. Rheumatol.* **2010**, *24*, 769–781. [CrossRef] [PubMed]
8. Traeger, A.C.; Buchbinder, R.; Elshaug, A.G.; Croft, P.R.; Maher, C.G. Care for low back pain: Can health systems deliver? *Bull. World Health Organ.* **2019**, *97*, 423–433. [CrossRef] [PubMed]
9. Kheirinejad, S.; Visuri, A.; Suryanarayana, S.A.; Hosio, S. Exploring mHealth applications for self-management of chronic low back pain: A survey of features and benefits. *Heliyon* **2023**, *9*, e16586. [CrossRef] [PubMed]
10. Aspden, R. A new mathematical model of the spine and its relationship to spinal loading in the workplace. *Appl. Ergon.* **1988**, *19*, 319–323. [CrossRef]
11. Ferguson, S.J.; Steffen, T. Biomechanics of the aging spine. *Eur. Spine J.* **2003**, *12* (Suppl. 2), S97–S103. [CrossRef]
12. Iorio, J.A.; Jakoi, A.M.; Singla, A. Biomechanics of Degenerative Spinal Disorders. *Asian Spine J.* **2016**, *10*, 377–384. [CrossRef]
13. Esperança Pina, J.A. *Anatomia Humana da Locomoção*, 5th ed.; LIDEL—Edições Técnicas, lda: Lisbon, Portugal, 2014.
14. Seeley, R.; Stephens, T.; Tate, P. *Anatomia e Fisiologia*, 6th ed.; McGraw-Hill: New York, NY, USA, 2003.
15. Wolfla, C.; Stemper, B.; Board, D.; Yoganandan, N. Biomechanical properties of human thoracic spine disc segments. *J. Craniovertebral Junction Spine* **2010**, *1*, 18–22. [CrossRef]
16. Najm, W.I.; Seffinger, M.A.; Mishra, S.I.; Dickerson, V.M.; Adams, A.; Reinsch, S.; Murphy, L.S.; Goodman, A.F. Content validity of manual spinal palpatory exams—A systematic review. *BMC Complement. Altern. Med.* **2003**, *3*, 1. [CrossRef]
17. González, A.B.; Darby, S. Risk of cancer from diagnostic X-rays: Estimates for the UK and 14 other countries. *Lancet* **2004**, *363*, 345–351. [CrossRef]

18. Pinel-Giroux, F.-M.; Mac-Thiong, J.-M.; de Guise, J.A.; Berthonnaud, É.; Labelle, H. Computerised assessment of sagittal curvatures of the spine: Comparison between Cobb and tangent circles techniques. *J. Spinal Disord. Tech.* **2006**, *19*, 507–512. [CrossRef]
19. Harlick, J.C.; Milosavljevic, S.; Milburn, P.D. Palpation identification of spinous processes in the lumbar spine. *Man. Ther.* **2007**, *12*, 56–62. [CrossRef] [PubMed]
20. Moura, D.C.; Boisvert, J.; Barbosa, J.G.; Labelle, H.; Tavares, J.M.R. Fast 3D reconstruction of the spine from biplanar radiographs using a deformable articulated model. *Med. Eng. Phys.* **2011**, *33*, 924–933. [CrossRef] [PubMed]
21. Brink, Y.; Louw, Q.; Grimmer-Somers, K. The quality of evidence of psychometric properties of three-dimensional spinal posture-measuring instruments. *BMC Musculoskelet. Disord.* **2011**, *12*, 93. [CrossRef] [PubMed]
22. Greendale, G.A.; Nili, N.S.; Huang, M.-H.; Seeger, L.; Karlamangla, A.S. The reliability and validity of three non-radiological measures of thoracic kyphosis and their relations to the standing radiological Cobb angle. *Osteoporos. Int.* **2011**, *22*, 1897–1905. [CrossRef] [PubMed]
23. Coelho, D.M.; Bonagamba, G.H.; Oliveira, A.S. Scoliometer measurements of patients with idiopathic scoliosis. *Braz. J. Phys. Ther.* **2013**, *17*, 179–184. [CrossRef] [PubMed]
24. Giglio, C.A.; Volpon, J.B. Development and evaluation of thoracic kyphosis and lumbar lordosis during growth. *J. Child. Orthop.* **2007**, *1*, 187–193. [CrossRef] [PubMed]
25. Mirbagheri, S.-S.; Rahmani-Rasa, A.; Farmani, F.; Amini, P.; Nikoo, M.-R. Evaluating kyphosis and lordosis in students by using a flexible ruler and their relationship with severity and frequency of thoracic and lumbar pain. *Asian Spine J.* **2015**, *9*, 416–422. [CrossRef]
26. Mannion, A.F.; Knecht, K.; Balaban, G.; Dvorak, J.; Grob, D. A new skin-surface device for measuring the curvature and global and segmental ranges of motion of the spine: Reliability of measurements and comparison with data reviewed from the literature. *Eur. Spine J.* **2004**, *13*, 122–136. [CrossRef]
27. Vutan, A.-M.; Lovasz, E.-C.; Amarandei, M.; Ciupe, V. The methods used for the diagnosis and evaluation of scoliosis. *Timis. Phys. Educ. Rehabil. J.* **2016**, *9*, 36–41. [CrossRef]
28. Quaresma, C.; João, F.; Fonseca, M.; Secca, M.F.; Veloso, A.; O'neill, J.G.; Branco, J. Comparative evaluation of the tridimensional spine position measured with a new instrument (Vertebral Metrics) and an optoelectronic system of stereophotogrammetry. *Med. Biol. Eng. Comput.* **2010**, *48*, 1161–1164. [CrossRef]
29. Gabriel, A.; Quaresma, C.; Vieira, P. Vertebral metrics—Automation of a non-invasive instrument to analyse the spine. In *BIODEVICES 2015—8th International Conference on Biomedical Electronics and Devices, Proceedings of the 8th International Joint Conference on Biomedical Engineering Systems and Technologies, BIOSTEC 2015, Lisbon, Portugal, 12–15 January 2015*; Cliquet, A., Jr., Fred, A., Gamboa, H., Elias, D., Eds.; SciTePress—Science and Technology Publications: Setúbal, Portugal, 2015; pp. 150–155.
30. Gabriel, A.T.; Quaresma, C.; Secca, M.F.; Vieira, P. Development and clinical application of Vertebral Metrics: Using a stereo vision system to assess the spine. *Med. Biol. Eng. Comput.* **2018**, *56*, 1435–1446. [CrossRef] [PubMed]
31. Gruescu, C.M.; Garaiman, A.; Lovasz, E.C. Modeling of human spinal column and simulation of spinal deformities. *Mechanika* **2015**, *21*, 214–219. [CrossRef]
32. Campbell-Kyureghyan, N.; Jorgensen, M.; Burr, D.; Marras, W. The prediction of lumbar spine geometry: Method development and validation. *Clin. Biomech.* **2005**, *20*, 455–464. [CrossRef]
33. Lavecchia, C.E.; Espino, D.M.; Moerman, K.M.; Tse, K.M.; Robinson, D.; Lee, P.V.S.; Shepherd, D.E.T. Lumbar model generator: A tool for the automated generation of a parametric scalable model of the lumbar spine. *J. R. Soc. Interface* **2018**, *15*, 20170829. [CrossRef] [PubMed]
34. Panjabi, M.M. Three-dimensional mathematical model of the human spine structure. *J. Biomech.* **1973**, *6*, 671–680. [CrossRef]
35. Boisvert, J.; Cheriet, F.; Pennec, X.; Labelle, H.; Ayache, N. Principal Deformations Modes of Articulated Models for the Analysis of 3D Spine Deformities. *Electron. Lett. Comput. Vis. Image Anal.* **2008**, *7*, 13–31. [CrossRef]
36. Poredoš, P.; Čelan, D.; Možina, J.; Jezeršek, M. Determination of the human spine curve based on laser triangulation. *BMC Med. Imaging* **2015**, *15*, 2. [CrossRef] [PubMed]
37. Panjabi, M.M.; Duranceau, J.; Goel, V.; Oxland, T.; Takata, K. Cervical human vertebrae quantitative three-dimensional anatomy of the middle and lower regions. *Spine* **1991**, *16*, 861–869. [CrossRef]
38. Panjabi, M.M.; Takata, K.; Goel, V.; Federico, D.; Oxland, T.; Duranceau, J.; Krag, M. Thoracic human vertebrae quantitative three-dimensional anatomy. *Spine* **1991**, *16*, 888–901. [CrossRef] [PubMed]
39. Panjabi, M.M. The stabilizing system of the spine. Part I. Function, dysfunction, adaptation, and enhancement. *J. Spinal Disord.* **1992**, *5*, 383–389. [CrossRef] [PubMed]
40. Yu, H.; Wilamowski, B.M. *The Industrial Electronics Handbook—Intelligent Systems*, 2nd ed.; CRC Press: Boca Raton, FL, USA, 2011.
41. Moll, J.M.; Wright, V. New York clinical criteria for ankylosing spondylitis. A statistical evaluation. *Ann. Rheum. Dis.* **1973**, *32*, 354–363. [CrossRef] [PubMed]
42. Akgul, O.; Ozgocmen, S. Classification criteria for spondyloarthropathies. *World J. Orthop.* **2011**, *2*, 107–115. [CrossRef]
43. Jang, J.H.; Ward, M.M.; Rucker, A.N.; Reveille, J.D.; Davis, J.C.; Weisman, M.H.; Learch, T.J. Ankylosing spondylitis: Patterns of radiographic involvement—A re-examination of accepted principles in a cohort of 769 patients. *Radiology* **2011**, *258*, 192–198. [CrossRef] [PubMed]

44. Baraliakos, X.; Listing, J.; Brandt, J.; Haibel, H.; Rudwaleit, M.; Sieper, J.; Braun, J. Radiographic progression in patients with ankylosing spondylitis after 4 yrs of treatment with the anti-TNF-α antibody infliximab. *Rheumatology* **2007**, *46*, 1450–1453. [CrossRef]
45. Ramiro, S.; Stolwijk, C.; van Tubergen, A.; van der Heijde, D.; Dougados, M.; Van den Bosch, F.; Landewé, R. Evolution of radiographic damage in ankylosing spondylitis: A 12 year prospective follow-up of the OASIS study. *Ann. Rheum. Dis.* **2015**, *74*, 52–59. [CrossRef]
46. Singer, K.P.; Edmondston, S.J.; Day, R.E.; Breidahl, W.H. Computer-Assisted Curvature Assessment and Cobb Angle Determination of the Thoracic Kyphosis—An In Vivo and In Vitro Comparison. *Spine* **1994**, *19*, 1381–1384. [CrossRef]
47. Hanneman, S.K. Design, Analysis, and Interpretation of Method-Comparison Studies. *AACN Adv. Crit. Care* **2008**, *19*, 223–234. [CrossRef]
48. Doğan, N. Bland-Altman analysis: A paradigm to understand correlation and agreement. *Turk. J. Emerg. Med.* **2018**, *18*, 139–141. [CrossRef]
49. Giavarina, D. Understanding Bland Altman analysis. *Biochem. Medica* **2015**, *25*, 141–151. [CrossRef]
50. Picone, V.; Makris, N.; Boutevin, F.; Roy, S.; Playe, M.; Soussan, M. Clinical validation of time reduction strategy in continuous step-and-shoot mode during SPECT acquisition. *EJNMMI Phys.* **2021**, *8*, 10. [CrossRef]
51. Thirunavukarasu, A.J.; Mullinger, D.; Rufus-Toye, R.M.; Farrell, S.; Allen, L.E. Clinical validation of a novel web-application for remote assessment of distance visual acuity. *Eye* **2022**, *36*, 2057–2061. [CrossRef]
52. Azram, M.; Ahmed, N.; Leese, L.; Brigham, M.; Bowes, R.; Wheatcroft, S.B.; Ngantcha, M.; Stegemann, B.; Crowther, G.; Tayebjee, M.H. Clinical validation and evaluation of a novel six-lead handheld electrocardiogram recorder compared to the 12-lead electrocardiogram in unselected cardiology patients (EVALECG Cardio). *Eur. Heart J.-Digit. Health* **2021**, *2*, 643–648. [CrossRef] [PubMed]
53. Merchant, M.; Parfenov, A.; Bettencourt, A.; Klein, L. Clinical Validation of Non-Invasive Monitor Of Hemodynamic Congestion In Heart Failure Patients. *J. Card. Fail.* **2023**, *29*, 557. [CrossRef]
54. Ghafari, C.; Houissa, K.; Dens, J.; Ungureanu, C.; Kayaert, P.; Constant, C.; Carlier, S. Clinical Validation of a New Enhanced Stent Imaging Method. *Algorithms* **2023**, *16*, 276. [CrossRef]
55. Hadjidimitriou, S.; Pagourelias, E.; Apostolidis, G.; Dimaridis, I.; Charisis, V.; Bakogiannis, C.; Hadjileontiadis, L.; Vassilikos, V. Clinical Validation of an Artificial Intelligence–Based Tool for Automatic Estimation of Left Ventricular Ejection Fraction and Strain in Echocardiography: Protocol for a Two-Phase Prospective Cohort Study. *JMIR Res. Protoc.* **2023**, *12*, e44650. [CrossRef]